

Experimental optimization environment for developing an intracycle pitch control in cross flow turbines

Stefan HOERNER, Roberto LEIDHOLD, Shokoofeh ABBASZADEH, Karla RUIZ-HUSSMANN, Timo BENNECKE, Zhao ZHAO, Paul JOEDECKE, Christian-Toralf WEBER, Pierre-Luc DELAFIN, Cyrille BONAMY and Yves DELANNOY

Abstract—Cross-flow tidal turbines have not reached the efficiency of horizontal-axis turbines. Among various improvement approaches found in the literature, the intracycle pitch control is one of the most promising ones. It consists in actively pitching each blade as function of the azimuth angle. This paper presents the development of an experimental environment to optimize the intracycle control for cross-flow tidal turbines, the aim of the project OPTIDE, a collaboration of the Otto-von-Guericke-University Magdeburg, Germany, the University Grenoble-Alpes in France and the University of Applied Sciences Magdeburg-Stendal. The experimental system consists of a turbine flume model equipped with a controlled generator. The three bladed turbine will have independently controlled pitch actuators embedded in each blade with a force sensing system. Local high dynamic systems control the speed of the generator and the pitch position as a function of the azimuth angle. A superimposed governing system performs an experimental optimization process. Evolutionary algorithms are to be employed to solve two objectives: (1) maximizing the efficiency and (2) minimizing the structural loads. These kind of problems are usually solved with numerical simulations, which commonly comes with very high computational efforts and uncertainty. For this reason simulations are replaced by an experimental optimization technique. It is expected that this method could quickly

and reliably find optimal pitch trajectories once the setup is fully installed. In the course of the project selected cases will be analysed using particle-image velocimetry (PIV) with synchronized force measurements to research the hydrodynamic mechanisms and the effects of the flow control performed by the pitching motion. In this paper we provide an overview over the decision and design process of the experimental flume setup and the project goals.

Index Terms—Vertical axis tidal turbines, instrumentation, optimization, control, experiments, CFD

I. INTRODUCTION

TIDAL energy has a huge potential to contribute to the immense technological challenges arising from the worldwide transition towards carbon free societies within the next decades. Together with wave and marine flows, tidal streams provide the largest sources of renewable energy globally. This is further underlined by their great abundance, their reliability and predictable nature as pointed out by Holzmann *et al.* 2007 [1], Angeloudis *et al.* 2016 [2], or Neil *et al.* 2018 [3]. Tides are based on lunar and planetary motion which can easily be predicted with great accuracy. Furthermore they are largely unaffected by climate change and weather.

When implemented at large scale, tidal turbines can substantially contribute to solve the European grid stability problem by providing to the base load supply. Thus, they can become a key driver for the transition to carbon-free energy generation. In contrast to wind and solar which are highly stochastic and challenging for Europe's power infrastructure (see Kyesswa *et al.* 2020 [4] or Urbanek *et al.* 2019 [5]) the predictable and reliable nature of tidal, marine and river currents makes them ideal providers of baseload power generation. In addition, thanks to their highly controllable characteristics they can be exploited as a demand side response, which improves the agility and resilience of the energy market as a whole. This allows for a replacement of both fossil fired gas turbines as well as fossil and nuclear power heated steam-electric power plants without the constraint of the typical and significant losses from power-to-hydrogen conversion methods resulting in storage efficiencies of 50-65% if the entire process is accounted as noted by Zapf 2017 [6].

Limiting factors for a broad exploitation of marine hydropower technologies are commonly based on their footprint at sea bed, ecological impacts and societal

Part of a special issue for EWTEC 2023. Original version published in EWTEC 2023 proceedings at <https://doi.org/10.36688/ewtec-2023-578>.

Manuscript submitted 16 December 2024; Accepted 13 January 2025. Published 31 May 2025

This is an open access article distributed under the terms of the Creative Commons Attribution 4.0 International license. CC BY <https://creativecommons.org/licenses/by/4.0/>.

This paper has been subjected to single-blind peer review by a minimum of two reviewers.

This work is part of the OPTIDE project and has been supported by the Deutsche Forschungsgemeinschaft (DFG (FKZ: 457325924)) and the labex Tec21 Investissements d'avenir - agreement n°ANR-11-LABX-0030.

S. Hoerner and K. Ruiz-Hussmann are affiliated at both the Univ. Grenoble Alpes, CNRS, Grenoble INP, LEGI, Grenoble, France and the Institute of Fluid Dynamics and Thermodynamics at Otto von Guericke University, Magdeburg, Germany (e-mail: stefan.hoerner@univ-grenoble-alpes.fr)

R. Leidhold, S. Abbaszadeh and Z. Zhao are with the Institute of Electrical Power Systems, OVGU Magdeburg, Germany.

T. Bennecke is researcher at the Institute of Fluid Dynamics and Thermodynamics at Otto von Guericke University (OVGU) Magdeburg, Universitätsplatz 2, 39106 Magdeburg, Germany

P. Joedecke was at the Department of Engineering and Industrial Design, University of Applied Sciences Magdeburg-Stendal, Magdeburg, Germany.

C.-T. Weber is currently at the Department of Engineering and Industrial Design, University of Applied Sciences Magdeburg-Stendal, Magdeburg, Germany.

P.-L. Delafin, C. Bonamy and y. Delannoy are researchers at the Univ. Grenoble Alpes, CNRS, Grenoble INP, LEGI, Grenoble, France. Digital Object Identifier: <https://doi.org/10.36688/imej.8.37-46>

challenges such as conflicts of use or local acceptance, as well as high levelized costs of electricity (LCOE) compared to other renewable sources such as wind or solar. Suitable marine hydropower sites are expected to remain in limited supply. This is due to flow conditions, but also to conflicts with ecology, the naval industry, transport, cultural heritage and tourism as shown by Barnier *et al.* 2020 [7] and Bugnot *et al.* 2020 [8]. It is therefore critical that such a valuable environment like the seafloor is optimally used with lowest impact on its environment.

Hydrokinetic cross-flow-tidal turbines (CFTT) can provide suitable solutions for many of the technological challenges which can be derived from the above mentioned constraints, as their operating principle only exploits the in-stream energy of a tidal or marine current. In consequence no hydraulic head achieved by guiding structures or vast installations such as dams are necessary for their operation.

Beyond other, in particular three key advantages of CFTT can be identified:

(1) Ecological impacts: fish and other aquatic life forms, such as sea mammals, are able to avoid collisions, as shown by Zhang *et al.* 2017 [9] or Müller *et al.* 2023 [10]. Most concerns are rising on possible influences on the behavior of fish, like avoidance of former habitats or migration routes, as shown by Berry *et al.* 2019 [11] or Castro-Santos *et al.* 2015 [12]. There remains a clear need for further investigation on the detailed ecological impacts of these technologies. However they can be considered to be of significant lower impact compared to conventional tidal hydropower facilities such as the *La Rance* station in France.

(2) Energy costs: due to the absence of dams or other large technical installations, the initial investments are low, even though underwater installations, such as cable installations or mooring, are highly expensive due to the harsh offshore environment. However, regarding the levelized costs of electricity (LCOE), EU's Strategic Energy Technology Plan (SET) has set cost-reduction targets for 2030 to 0.10 EUR/kWh for tidal energy¹, which is on the lower level of the LCOE of carbon and gas driven plants (which can be replaced by these technologies) but far beyond the lowest LCOE of wind and solar with roughly 0.03-0.04 €/kWh in 2021 as reported by the Fraunhofer society [13].

(3) Land use: coasts and littorals are the most populated areas worldwide with immense economical and ecological importance. In consequence, the area based power density is key for a successful take off of emerging tidal energy technologies. CFTT provide a magnitude higher area-based power density compared to axial turbines which are commonly employed in wind industry, as initially modeled by Whittlesey *et al.* 2010 [14] based on a bioinspired fish schooling approach and subsequently confirmed in field tests by Dabiri *et al.* 2011 [15] on a wind turbine farm. According to Brownstein *et al.* 2016 [16], these increased area based efficiency is due to a positive inter-turbine interaction.

These strengths and advantages of CFTT are counter balanced by quite low single turbine efficiencies, complex flow patterns in the rotors and alternating blade loads during each rotation, which can lead to fluid-induced vibrations and material fatigue. The origin of these drawbacks is in what Le Fouest & Mulleners 2022 [17] called the *dynamic stall dilemma*.

A. CFTT and complex fluid dynamics

The process of dynamic flow separation and re-attachment, so-called dynamic blade stall, plays a significant role for the operation of CFTT. These effects are dominant in particular for operating conditions featuring low tip-to-speed ratios expressed by $\lambda = \frac{v_{\text{blade}}}{v_{\infty}} < 2$, while v_{blade} is the tangential speed of the blade equivalent to the circumferential rotor speed and v_{∞} is the absolute flow velocity far from the turbine. Low relative rotational speed operating regimes are advantageous for the efficiency of rotors with high solidity. They have been extensively researched e.g. by Shiono *et al.* 2000 [18] or Delafin *et al.* 2016 [19]. This high solidity is commonly the case for hydraulic machinery due to high density of water, compared to air, which makes wind turbines from a finer and thinner structural design. Blade stall dependencies on the operating point are due to the angle of attack α which varies in great bandwidth as a function of the operation point λ and azimuth angle (θ):

$$\alpha = \arctan\left(\frac{\sin\theta}{\lambda + \cos\theta}\right) \quad (1)$$

Following McCroskey *et al.* 1981 [20] two crucial parameters for the onset and the character of dynamic stall can be determined in a dynamic system with variations of α and flow speed: the effective maximum angle of attack on the blade α and the relation of the time scale of a possible vortex generation (from the change rate of the angle of attack $\dot{\alpha}$) and the time scale required to convect such a vortex over the blade surface. This relation is mostly denoted as the reduced frequency k . McCroskey defined k for helicopters in a static reference frame (eq. (2 left)) with respect to v_{∞} . This was extended to a rotating reference by Laneville *et al.* 1986 [21] (eq.(2 right)):

$$k = \frac{C \cdot \dot{\alpha}_{\text{max}}}{2v_{\infty} \cdot \alpha_{\text{max}}} = \frac{C \cdot \dot{\alpha}_{\text{max}}}{2\omega \cdot R \cdot \alpha_{\text{max}}} \quad (2)$$

While C is the chord length and R is the radius. Laneville *et al.* also redefined k for a CFTT. To this effect, eqs. (1) and its derivation for $\dot{\alpha}$ are inserted in eq. (2 right). It should be noted that the maximum of the absolute value of $\dot{\alpha}$ is of interest:

$$k = \frac{C}{2 \cdot R \cdot (\lambda - 1) \cdot \arctan\left[(\lambda^2 - 1)^{-\frac{1}{2}}\right]} \quad (3)$$

As shown in the aforementioned equations, λ and α are the two key parameters for the flow regime at blade level.

The best operating point (λ_{best}) is a trade-off in between stall effects (which diminish with increasing λ) and other losses dominated by the the structural

¹https://energy.ec.europa.eu/topics/renewable-energy/offshore-renewable-energy_en

strength (solidity) of the structure and the number of blades. A decrease of λ_{best} can be found along with increasing number of blades and increasing structural solidity. This is due to effects from blade interactions (increase with λ) and losses from the support structure from rising rotational speed and thickness of the structure. These losses non-linearly grow with λ^2 or even λ^3 as reported by Daróczy *et al.* 2015 [22].

In order to reduce the torque ripple most of the current systems feature at least two, often three blades, e.g. Maître *et al.* 2014 [23], Daróczy *et al.* 2018 [24] or Chen *et al.* 2022 [25].

To summarize λ_{best} is not an arbitrarily selectable parameter. In consequence the bandwidth for a variation of λ seems limited and other measures for a stall inhibition or mitigation should be prioritized.

Bio-inspired approaches using specific blade shapes, such as leading edge tubercles, have been reported for stall mitigation and flow control by Hansen *et al.* 2016 [26] or Pérez-Torró & Kim 2017 [27]. Another approach to handle the stall dilemma on a CFTT is to control α .

Multiple methods have been investigated so far:

- (1) A direct control of the maximum angle of attack α using an active pitch actuation or blade morphing, a recent review is given by Rathore *et al.* 2021 [28]
- (2) A passive control of α by pitch mechanisms (e.g. Lazauskas & Kirke 2012 [29]) or blade morphing driven from hydrodynamic forces, such as flexible blades as shown by Hoerner *et al.* 2019 [30] & 2021 [31] or Descoteaux & Olivier 2021 [32]
- (3) An intracycle control of the angular velocity, which changes α implicitly over the resulting speed triangles as shown by Strom *et al.* 2017 [33]

Within this study an optimized pitching law for an actuated blade pitch approach is investigated.

B. OPTIDE project

The *experimental and numerical OPTimization of a cross-flow TIDal turbinE (OPTIDE)* project aims for an experimental proof and quantification of the increases of turbine efficiency and mitigation of structural loads in CFTT from intracycle pitch control predicted on numerically studies (such as Paillard *et al.* 2015 [34] or Delafin *et al.* 2021 [35]) or based on experimental surrogate models (such as Abbaszadeh *et al.* 2019 [36]).

Existing studies are mostly based on numerical findings or provide only poor quantitative improvements as the actuation or transmission systems were obstructing the flow and led themselves to significant flow perturbations. It is hypothesized that fluid-induced vibrations and dynamic stall can be mitigated by means of such an intracycle blade pitch in accordance to the findings of the aforementioned studies. In consequence a systematically optimized active flow control strategy using a blade-embedded highly dynamic actuation system is to be developed. The interdisciplinary project is a close collaboration of scientists from Germany (Otto von Guericke University Magdeburg and University of Applied Sciences Magdeburg) and France (LEGI labs, University Grenoble Alpes).

The project methodology and the state of project will be reported subsequently in detail.

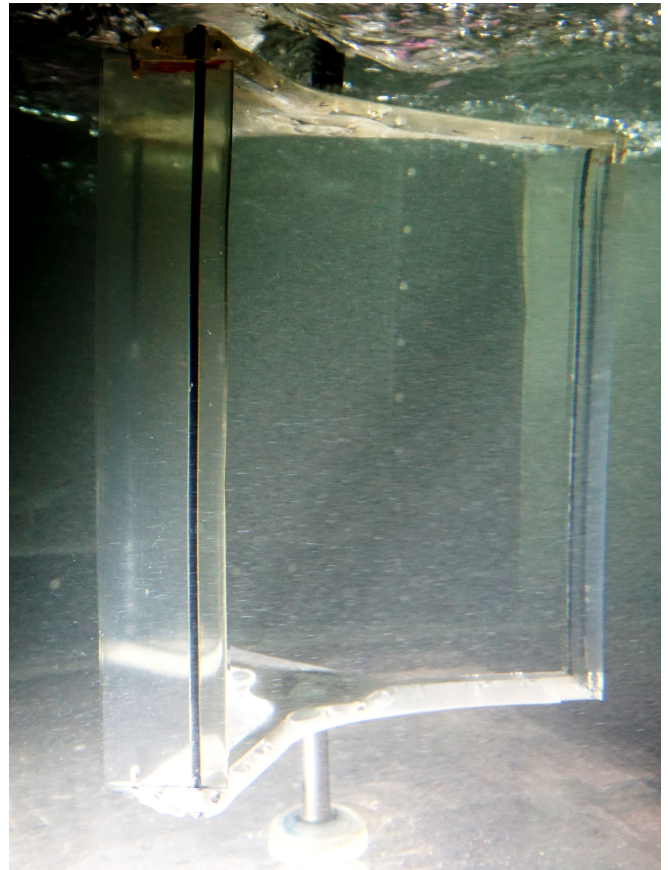


Fig. 1. The flume model has a hybrid design from a aluminum skeleton and a 3D printed shell structure. The size of $400 \times 400 \text{ mm}^2$ is a tradeoff in between the constraints from the blade-embedded actuation system, the chord based turbulence level and confinement from flow blockage. (The picture has been rectified in order correct lens aberrations)

II. METHODOLOGY

A. Flume model development

The turbine model (as shown in fig. 1) is dedicated to operate in a lab flume at Otto von Guericke University Magdeburg with a cross section of $1200 \times 600 \text{ mm}^2$. The maximum flow velocity for a water level of 600 mm is around 0.7 m/s. Reynolds similarity and a reasonable size of the mechatronical system require to scale up the machine to a diameter of about 1000 mm in order to operate under a blade-based Reynolds number (Re) $> 10^6$ to be able reach flow similarity with machines in a fully turbulent environment such as in the sea.

In opposition, in order to avoid a significant effect or dominance of the confinement effects from a blockage ratio > 0.1 it is required to scale down the turbine to a diameter of about 300 mm for a aspect ratio of 1.

In a trade off in between those physical constraints and with respect to the size of the blade-embedded actuation system, the three-bladed turbine model was designed with a diameter and blade length of 400 mm (aspect ratio 1) and a chord length of roughly 70 mm. This leads to a solidity $\sigma = \frac{nC}{R}$ of 1.05 (with n the number of blades). The turbulence level (Re) at the blade will vary in a bandwidth from 70,000 to 210,000 with an average of 140,000. The variation is a consequence of the rotation axis situated perpendicular to the freestream. The confinement of 22% will still have

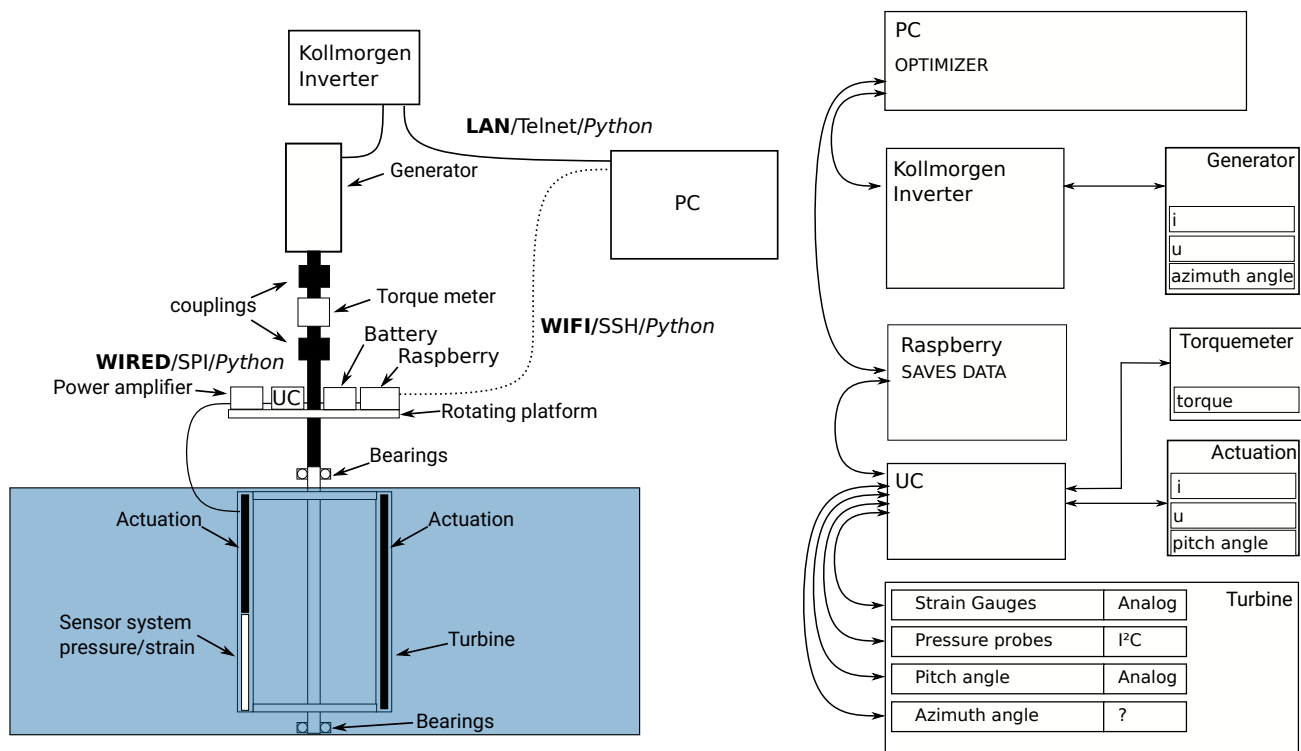


Fig. 2. The OPTIDE project aims for an optimized pitch mechanism and control for CFTT. With respect to the complex flow regimes in the rotor an experimental optimization approach is developed. To this purpose genetic algorithms are coupled with a fully automatized experimental setup in a experimental flume.

a serious and non-negligible effect on the performance as well as the free surface of the flume. It is planned to investigate and correct these impacts on the base of numerical studies.

B. Instrumentation concept

The aim of the optimization is to maximize the power output and to minimize structural loads and vibrations. To this purpose, the mechanical torque T and azimuth angle θ have to be captured (mechanical power) as well as the hydraulic blade loads in axial F_A and tangential F_T direction. F_T is contributing to the torque with the support arm as lever, while F_A will only generate (undesired) structural loads.

To capture the dynamics from the alternating flow regime, the sampling rate for the synchronous recording for the sensors devices has been set to 1 kHz. In a first version of the setup (as shown in fig. 1) the blades are not yet actuated. The torque T is captured using a classical torque meter (Lorenz Meßtechnik FM-G 30 NM) in the static lab frame. In a second phase (after definition of the necessary measurement range) it will be replaced by a rotating version read out by a microcontroller (TI-F28069). The position feedback from the load machine (power inverter Kollmorgen AKD-P00306 with Siemens 1fk7042-5af71-1ta0) is transferred as a quadrature signal and captured together with the torque using a Labjack T7 acquisition card. The inverter type allows for a fully automatized setup in a Python based experimental environment with a custom communication library developed and presented by Abbaszadeh *et al.* 2019 [36], where further

details can be found. A second position feedback for synchronization from rotating to fixed reference frame measurements will be placed on a rotating platform as well (see fig. 2). The flow speed at the inlet section has been once characterized using acoustic doppler velocimetry (Vectrino profiler). During the measurements the flow condition will be reproduced using the same settings for the inverter driven pumps of the flume. Laser doppler anemometry (LDA) measurements have shown that the repeatability of the flow conditions can be assured with a satisfying average deviation of $<1\%$. The forces will be captured using custom signal amplifiers using multiple strain gauges grouped to full bridges to compensate for interfering other forces and temperature elongation effects. Details of communication from rotating to static references will be discussed later. High speed 2D-2-components particle image velocimetry (PIV) will be performed on the reference turbine and on the actuated version with intracycle blade pitch.

C. Investigations of the fluid-structure interactions

In order to achieve a lightweight design with adequate strength for the flume model and with respect to the complex instrumentation, a fluid-structure interaction (FSI) study was conducted prior to the manufacturing of the model (see fig. 3).

The strain gauges which are used for the single blade load measurements require a decent deformation of the structure. Consequently, the structure has been weakened where the gauges are placed to achieve an

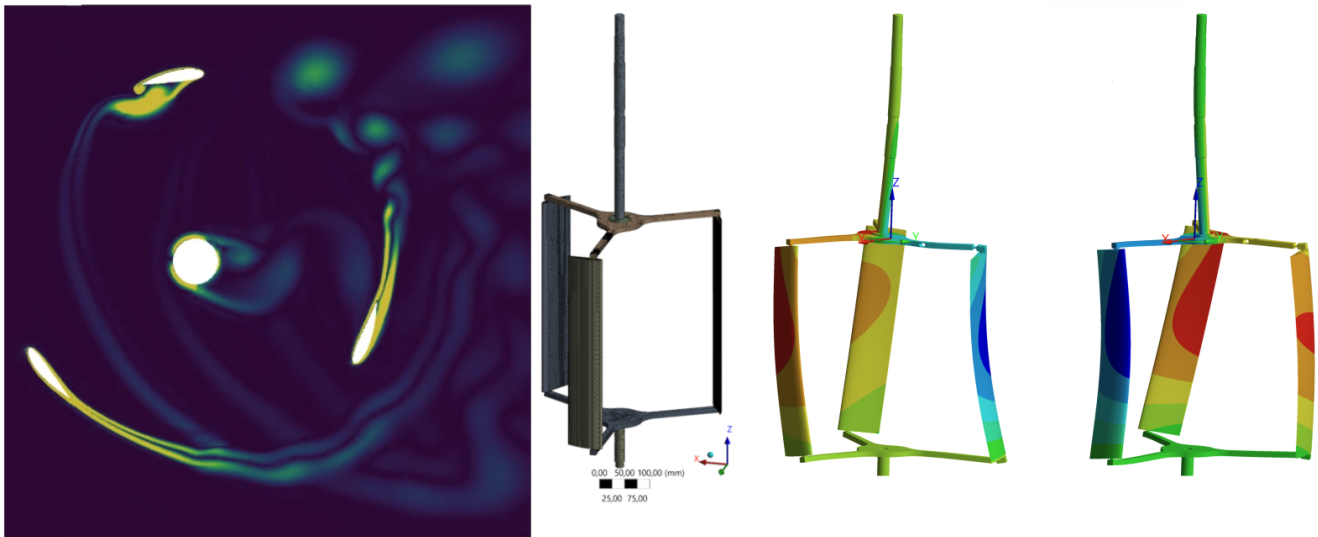


Fig. 3. A weak coupled FSI study (CFD: OpenFOAM v2212, FEA: Ansys WorkBench 22R2 custom coupling approach) was conducted to approve the structural design and the instrumentation of the flume model. (left) Numerical simulations of the flow in a CFTT, borrowed from Hoerner *et al.* 2021 [31]; (middle and right) FE analysis of the structural displacement for two azimuth angles. Details on the methodology are provided by Bennecke *et al.* 2022 [37] & 2023 [38]

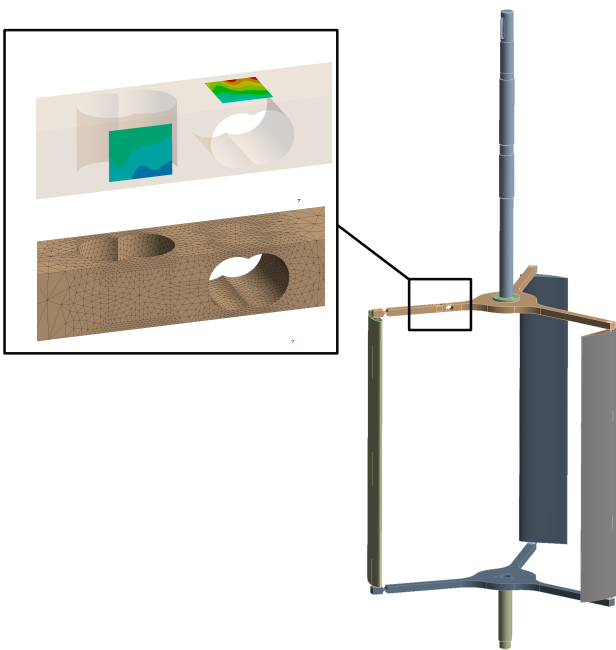


Fig. 4. Instrumentation of the turbine with strain gauges. To obtain an adequate signal from the strain gauges, the blade supports were weakened. The design is based on two full bridges. One each for tangential and normal (radial) force components. The material weakening was calculated using the simulated strains from the FSI analysis. The analysis also showed that additional instrumentation is necessary to measure the single blade loads [38].

adequate signal (see fig. 4). However, if the structure becomes too weak, fluid-induced vibrations would have an undesired impact on the measurements and even may harm the rotor. As the deformation remain *small*, no direct effect on the flow field is expected. This allows for a weak coupled segregated or also called partitioned approach that maps the fluid induced forces retrieved from computational fluid mechanics (CFD) to a finite-element analysis (FEA) and

subsequently allows for a deformation and structural strength analysis of a given structure.

In the case at hand, the numerical simulations were performed with use of the open-source multiphysics toolkit OpenFOAM (v.2212 ESI fork) by the French project partners using 2D URANS simulations with a $k-\omega$ SST turbulence model and resolved boundary layer ($y^+ < 1$) following the CFD best practice guidelines. The setup is the same as used in Delafin *et al.* 2019 [39]. The unsteady 2D pressure distribution on the blade section was subsequently transferred in a transient 3D FEA by an extrusion of the values along the blade length as an imported load using Ansys Workbench (2020 R2) in a joint workgroup of the two Universities at Magdeburg. Details of the FSI study can be found in Bennecke *et al.* 2022 [37].

The hybrid design approach using an aluminum skeleton (water jet cut pieces from plates and standardized elements) with 3D printed shells (clear resin printer Formlabs 3I) for a flow optimized shape could be approved. It allows for changes of the outer shell in a simple manner without further impacts on the system characteristics, such as weight or inertia. Furthermore it allows for conservation of the measurement concept even if parts of the design, such as the blades are changed. This concept was chosen in order to provide a multipurpose CFTT test bench for further investigations in future. A second purpose for the FSI studies was to approve the measurement concept for the strain gauges. It could be shown, that additional measures have to be taken to avoid interfering loads from other blades as presented by Bennecke *et al.* 2023 [38] in detail.

D. Actuator and control design

A particular and truly interdisciplinary challenge of the project is the blade-embedded actuation. Aforementioned CFD simulations from Delafin *et al.* 2021

[35] and experimental results from Hoerner *et al.* 2020 [40] and Abbaszadeh *et al.* 2019 [36] were used for a preliminary estimation of the required actuation power and torque. In a first step existing machines based on brushless DC (BLDC) motors with planet gearbox and a gear ratio of 64:1 (Faulhaber Type 1226 024B) have been selected in order to be operational and for a fast uptake of the experiments. These miniaturized drives feature a diameter of 12 mm (to fit in the blade). Due to the low torque and a undesirable backlash in the gears of up to 3°, it has been decided to install two motors per blade. This allows for an increase of the available torque and a compensation of the backlash as reported by Zhao *et al.* 2023 [41].

Each motor-pair is driven by a microcontroller (Texas Instrument F28069) with two power electronic converters i.e. power amplifiers (Texas Instrument BOOSTXL-DRV8323RH). A position control algorithm has been implemented in the microcontroller, using the motor-integrated position sensors as feedback. It is able to implement the intracycle pitch angle trajectory as function of the azimuth angle, as well as measure the pitch torque indirectly by means of the motor current.

These microcontrollers, one per blade, and one more to acquire additional variables, are placed on a rotating platform at the turbine (fig. 2 left) and are linked to a Raspberry Pi computer. The Raspberry Pi receives reference trajectories and returns measured variables from/to the stationary PC running the optimizer through wireless LAN. All the devices on the rotating platform are supplied by a LiPo battery.

Regarding the blade embedded actuators, further development is being carried out to increase the torque and get rid of the gearbox inherent backlash. For this purpose, limited angle torque motors (LATM) able to directly drive the blade without gearbox, are being researched as reported by Zhao *et al.* 2022 [42]. The main challenge is to design them, unlike traditional LATM, in a long and thin shape suitable to fit them in the blade.

E. Blade shape optimization

Even though the BLDC motors can be considered to be the smallest machines with satisfying performance available on the market, a 12 mm diameter is still a challenge for the blade design. Common CFTT from literature feature relative blade thicknesses of 12-18% of the chord length. However, with the aim to minimize the effort for the pitch actuation, the pivot point was placed at 0.25 of the chord length, at the aerodynamic center of the hydrofoil. This position is not commonly the thickest part of the profile. In consequence it has been decided to perform a blade shape optimization with aim to select the best possible blade shape with the constraint to fit the actuators at the given position.

The optimization approach is based on genetic algorithms, which will be discussed later in more detail, and a numerical evaluation of the designs. This means the use of the custom *Optimization Algorithm Library ++* (OPAL++)² developed at Otto von Guericke

University Magdeburg, which has been firstly introduced by Daróczy *et al.* 2014 [43] and has been used in several studies since, e.g. Daróczy *et al.* 2018 [24], Kerikous & Thévenin 2018 [44] or Parikh *et al.* 2022 [45]. In the present study OPAL++ was coupled with OpenFoam (v.2212 ESI fork) in 2D URANS simulations with similar settings as already mentioned in II-C.

However, for such a systematic optimization, a fully automatized setup is required. This means in particular the spatial discretization process. Here the OpenFoam utility blockMesh was chosen, as it allows for a full control in the generation of block-structured hexaedric meshes. The blockMesh utility is governed by a so-called dict-file, which is automatically generated for each individual during the optimization with Python scripts based on the profile shape determined from 8 coordinates and the variable chord length (selected by OPAL++) and the use of a Bézier-spline to generate a smooth blade curve. The multi-objective optimization aims for a maximization of the power output ($\max(C_P)$) and a minimization of the blade loads ($\min(f_\sigma)$). For f_σ a simple mechanical model of the rotor has been developed based on the assumption of a Bernoulli beam clamped on both ends for the blade. The stress factor f_σ has been defined to account for both the maximum stress amplitudes and the mean of the load, which is inspired from the approach used for the so-called Smith diagram for the avoidance of fatigue effects in structures.

The design space of 10 parameters (the chord length, λ and eight nodes for the profile) is expected to run around 800-1000 individuals before convergence and currently runs on the high performance cluster at the LEGI lab. Details on the methodology and the objectives can be found in Ruiz-Hussmann *et al.* 2022 [46] and 2023 [47]. At the end of the process a hydrofoil from the Pareto front will be chosen, which provides the best compromise in between power output and structural loads.

III. EXPERIMENTAL OPTIMIZATION

Computational fluid mechanics (CFD) are expensive from the non-linear character of their underlying physics. In consequence CFD simulations are either based on significantly simplified physics, such as the URANS method with fully modeled turbulence or very limited in their real world applicability, due to low realizable Reynolds numbers and investigation time scales, such as for direct Navier-Stokes (DNS) methods. Only these reductions allow to simulate a flow in a reasonable amount of time by iteratively solving the (mostly immense) equation systems. The resulting costs make engineers rather seeking for a *better* solution when solving a specific problem with fluid mechanical background, e.g. by a parametric study, than performing a systemic optimization which seeks for the *best* possible solution.

When employing a true systematic optimization based on CFD (CFD-O), several hundreds of single simulations for evaluation have to be performed to converge towards the best solution. This requires further simplifications such as a reduction to 2D (Kerikous

²see <https://wikis.ovgu.de/lss/doku.php?id=guide:opal>

& Thévenin 2018 [44]) or flow steadiness (Parikh *et al.* 2022 [45]), which negatively affects on the reliability and transferability of the results to the original problem. Even with these simplifications simulations can take weeks or month as reported by Cleynen *et al.* 2021 [48].

Keeping these limitations in mind, experimentally based optimizations (Exp-O) provide a promising alternative for many engineering problems. In particular for the optimization of control tasks, experiments can directly determine the best operating point such as done since years in maximum power point tracking (MPPT) for the determination of an instantaneous best operation point for wind turbines.

However the application of Exp-O techniques using a fully automatized hardware setup in the loop is much larger. In turbomachinery actuators can be used to morph a structure and shape optimization becomes possible. Complex trajectories can be investigated for the angular velocity in order to control the angle of attack as shown by Strom *et al.* 2017 [33] for a CFTT. Abbaszadeh *et al.* 2019 used an experimental surrogate model for a CFTT which allows for the research of multiple turbine configurations in single experimental setup (see. Hoerner *et al.* 2019 [30] for details) and investigated an optimized pitch trajectory for a CFTT in a full factorial approach. In this case the entire design space is investigated during an optimization, without any employment of more sophisticated mathematical optimization methods, such as gradient search to reduce the necessary computational or experimental evaluation effort. One trajectory was evaluated within seconds (Exp-O) instead of hours or even days (CFD-O). By sequentially testing the entire design space, the optimization converged after roughly one day. This approach has also inspired other groups to perform similar optimization methods, such as Fasse *et al.* 2023 [49], who optimized the pitch law for a Schneider-Voith propeller very recently in an experimental setup.

A. Optimization methods

Accounting for the small time required to evaluate a parameter set from the design space of an Exp-O, it is questionable if sophisticated optimization methods are always necessary. As mentioned before, Abbaszadeh *et al.* 2019 [36] investigated a design space with three free parameters in a full factorial approach in roughly one day after 340 parameter sets for a single objective: the maximization of the cycle-averaged turbine torque.

However, with aim to speed up the process for larger design spaces and multiple contradicting objectives it is reasonable to choose a faster but also robust method. For the OPTIDE project genetic algorithms were chosen to be most suitable as they are metaheuristic (problem independent) and the optimizer can be used as a black box coupled as a superior governing entity with a automatized setup.

In the present case the aforementioned custom optimizer from Otto von Guericke University OPAL++ is employed. It has been chosen as there is already a lot of experience with the package from former optimization

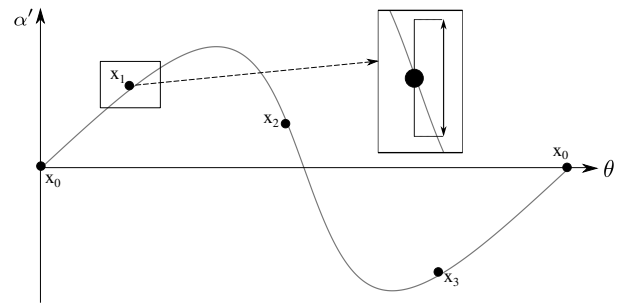


Fig. 5. The definition of the trajectory of the pitched angle of attack α' requires four nodes to define a suitable Bézier Spline.

studies using CFD-O. The coupling of the optimizer with the experiment is achieved using custom Python scripts which act as a communication layer with the microcontrollers (TI-F28069). As the optimization has multiple objectives the non-dominated sorting genetic algorithm II (NSGA-II) introduced by Deb *et al.* 2002 [50] will be chosen for its fast sorting capacities and robustness.

The three blades will perform the same trajectory (with 120° phase shift) for the pitched angle of attack α' . Inspired by the methodology of Abbaszadeh *et al.* 2019 [36] four parameters $x_0 - x_3$ will provide the nodes for a spline that defines the trajectory of α' (see fig. 5). The upper and lower limits of $x_0 - x_3$ are based on the analysis of the results from Delafin *et al.* 2021 [35] and Abbaszadeh *et al.* 2019 [36] to investigate a reasonable bandwidth and can later be proved by the results of the optimization.

OPAL++ will generate an initial population and all individuals will be evaluated sequentially. Each individual will initially run for 20 s to establish a periodic stable flow condition in the flume, which is equivalent to about 20 rotor turns. After this, 10 s of measurement time will be performed. Python scripts will evaluate the cycle-averaged power output (C_P) and the stress factor from blade loads (f_σ). This procedure will be performed in a loop until all individuals are evaluated and a new generation will be created by cross-over of the fittest individuals (for convergence) and mutation on the offspring (to cover the entire design space and to avoid local extrema). The process will be stopped when the objective space forms a sufficiently populated Pareto front.

B. Communication and experiment automation

As introduced in Sections II-B and II-D there are four microcontrollers on the rotating frame: three for controlling the pitch actuators and one additional for the sensors and data acquisition. The sensors are the strain gauges for axial and radial force measurements on one arm, a torque meter on the main shaft, and a position sensor also in the main shaft. The pitch controllers can also return the voltage, current, angle and the indirectly measured torque of the actuators. Regarding the real time algorithms in the microcontrollers, they are coded in C and can run with a 10 kHz sampling

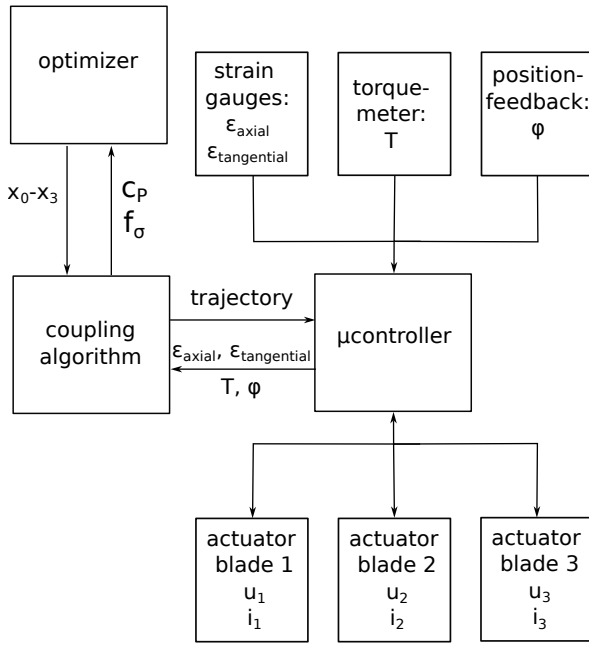


Fig. 6. Block diagram of the optimization functional blocks and information flow.

frequency, allowing for a high dynamic control and time resolution.

The four microcontrollers are linked to a Raspberry Pi computer through a 12 MBPS fast serial peripheral interface (SPI). The Raspberry Pi is the wireless LAN gateway to communicate with the computer implementing the optimizer. UDP protocol is used for the transfer of the relevant variables as follows: The optimizer sends the trajectory parameters $x_0 - x_3$ and the starting command for one optimization individual to the controllers. After the 30 s long test, as described in the previous section, the shaft torque, the shaft angle, the arm forces, as well as the pitch angle and torque as function of the azimuth angle are returned to the optimizer. A standard desktop PC is used to implement both, the coupling algorithm coded in Python and the OPAL++ optimization algorithm. It also provides a second measurement unit using the Labjack T7 acquisition card to capture the data from the generator.

In fig. 6 the optimization functional blocks and the information flow is depicted.

The speed-controlled load machine described in Section II-B gets the commands and parameters from the coupling algorithm, running in the desktop PC, via LAN using Telnet protocol. In a first stage of the project it will be used just to start, set a constant speed for the whole optimization process, and stop when finished. In a second stage, relying on the high dynamic control of the load machine, it will also be used for intracycle speed variation. The shaft position sensor on the stationary frame, used as feedback for the speed controller, generates also a pulse signal for triggering the PIV measurements at a given azimuth angle.

IV. PRELIMINARY RESULTS AND OUTLOOK

In the current state of the OPTIDE project numerical simulations have been performed for the flume model

design. A flume model with non-actuated NACA0018 blades (for reference) has been built and is now subject to a fluid mechanical characterization with synchronized torque and flow field measurements using high speed 2D2C PIV. The results will be used to validate CFD and FSI simulations (sec. II-E & II-C) and provide the base for a comparison with the latter fully actuated flume model with optimized blade shape and pitch trajectory (sec. III). In parallel the blade pitch control and actuation system has been developed and tested with success (sec. II-D).

A second version of the flume model is in the end phase of its design and build process. After completion of final water tightness tests, the actuated blades will be mounted along with the extended instrumentation using various microcontrollers in a custom setup placed on a rotating platform with wireless communication to the linux based governing system. This second phase flume model will provide a unique platform for the investigation of CFTT. The hybrid design based on an inner, instrumented aluminum support structure embedded in 3D printed shell elements allows for fast adaptations of the outer shell elements with negligible impact on inertia, weight or instrumentation of the turbine rotor. Therefore it is perfectly suitable for a direct comparison of design variations, e.g. for the systematic review of various blade shapes or the impact of other changes in geometry. This comes with the possibility to measure single blade loads in both axial and tangential component with high sampling rates and fully synchronized with power output and other parameters over the rotation angle.

In the course of the OPTIDE project the optimization of the pitch trajectory will be performed as soon as the second phase model is in place. Finally selected individuals from the Pareto Front will be investigated using the same approach as performed for the reference case using synchronized force and torque measurements combined with high speed PIV.

AUTHOR CONTRIBUTIONS

S.H.: Conceptualization, Methodology, Software, Resources, Writing - Original Draft, Supervision, Project administration, Funding acquisition. **R.L.** Conceptualization, Methodology, Software, Resources, Writing - Original Draft, Supervision, Project administration, Funding acquisition. **S.A.:** Conceptualization, Methodology, Software, Writing - Review & Editing. **K.R.H.:** Software, Formal analysis, Investigation, Data Curation, Visualization, Writing - Review & Editing. **T.B.:** Software, Formal analysis, Investigation, Data Curation, Visualization, Writing - Review & Editing. **Z.Z.:** Formal analysis, Investigation, Data Curation, Writing - Review & Editing. **P.J.:** Methodology, Formal analysis, Investigation, Writing - Review & Editing. **C.T.W.:** Supervision, Methodology, Formal analysis, Writing - Review & Editing. **P.L.D.:** Conceptualization, Methodology, Software, Resources, Writing - Review & Editing, Supervision, Project administration, Funding acquisition. **C.B.:** Conceptualization, Methodology, Software, Resources, Writing - Review & Editing, Supervision.

Y.D.: Conceptualization, Writing - Review & Editing, Supervision.

REFERENCES

- [1] D. C. Holzman, "Blue Power: Turning Tides into Electricity," *Environmental health perspectives*, vol. 115, no. 12, pp. A590–3, 2007.
- [2] A. Angeloudis, R. A. Falconer, S. Bray, and R. Ahmadian, "Representation and Operation of Tidal Energy Impoundments in a Coastal Hydrodynamic Model," *Renewable Energy*, vol. 99, pp. 1103–1115, 2016.
- [3] S. P. Neill, A. Angeloudis, P. E. Robins, I. Walkington, S. L. Ward, I. Masters, M. J. Lewis, M. Piano, A. Avdis, M. D. Piggott, G. Aggidis, P. Evans, T. A. Adcock, A. Židonis, R. Ahmadian, and R. Falconer, "Tidal Range Energy Resource and Optimization – Past Perspectives and Future Challenges," *Renewable Energy*, vol. 127, pp. 763–778, 2018.
- [4] M. Kyesswa, H. Cakmak, U. Kuhnappel, and V. Hagenmeyer, "Dynamic Modeling of Wind and Solar Power Generation with Grid Support for Large-Scale Integration in Power Systems," in *2020 IEEE PES Innovative Smart Grid Technologies Europe (ISGT-Europe)*. IEEE, 2020, pp. 569–573.
- [5] S. Urbanek, D. Heide, B. Bagaber, M. Lohss, B. Specht, X. Paulig, A. Mertens, and B. Ponick, "Analysis of External Rotor Electric Drives for an All-Automatic Airborne Wind Energy System," in *2019 IEEE International Electric Machines & Drives Conference (IEMDC)*. Piscataway, NJ: IEEE, 2019, pp. 1599–1606.
- [6] M. Zapf, *Power-to-Gas – Stand der Technik und Einsatzmöglichkeiten*. Wiesbaden: Springer Fachmedien Wiesbaden, 2017, pp. 165–265.
- [7] B. Barnier, A. Domina, S. Gulev, J.-M. Molines, T. Maître, T. Penduff, J. Le Sommer, P. Brasseur, L. Brodeau, and P. Colombo, "Modelling the impact of flow-driven turbine power plants on great wind-driven ocean currents and the assessment of their energy potential," *Nature Energy*, vol. 5, pp. 240–249, 2020.
- [8] A. Bugnot, M. Mayer-Pinto, L. Airolidi, E. C. Heery, E. L. Johnston, L. P. Critchley, E. M. A. Strain, R. L. Morris, L. H. L. Loke, M. J. Bishop, E. V. Sheehan, R. A. Coleman, and K. A. Dafforn, "Current and projected global extent of marine built structures," *Nature Sustainability*, 2020.
- [9] J. Zhang, D. Kitazawa, S. Taya, and Y. Mizukami, "Impact assessment of marine current turbines on fish behavior using an experimental approach based on the similarity law," *Journal of Marine Science and Technology*, vol. 22, no. 2, pp. 219–230, Jun 2017.
- [10] S. Müller, V. Muhawenimana, G. Sonnino-Sorisio, C. Wilson, J. Cable, and P. Ouro, "Fish response to the presence of hydrokinetic turbines as a sustainable energy solution," *Scientific Reports*, vol. 13, 05 2023.
- [11] M. Berry, J. Sundberg, and F. Francisco, "Salmonid response to a vertical axis hydrokinetic turbine in a stream aquarium," in *13th European Wave and Tidal Energy Conference (EWTEC)*, 2019.
- [12] T. Castro-Santos and A. Haro, "Survival and behavioral effects of exposure to a hydrokinetic turbine on juvenile atlantic salmon and adult american shad," *Estuaries and Coasts*, vol. 38, p. 203–214, 2015.
- [13] C. Kost, S. Shammugan, V. Fluri, D. Peper, A. D. Nemar, and T. Schlegl, "LCOE - renewable energy technologies," 2021. [Online]. Available: www.ise.fraunhofer.de/content/dam/ise/en/documents/publications/studies/EN2021_Fraunhofer-ISE_LCOE_Renewable_Energy_Technologies.pdf
- [14] R. Whittlesey, S. Liska, and J. Dabiri, "Fish schooling as a basis for vertical axis wind turbine farm design," *Bioinspiration & Biomimetics*, vol. 5, no. 3, p. 035005, 2010.
- [15] J. Dabiri, "Potential order-of-magnitude enhancement of wind farm power density via counter-rotating vertical-axis wind turbine arrays," *Journal of Renewable and Sustainable Energy*, vol. 3, no. 4, 2011.
- [16] I. Brownstein, M. Kinzel, and J. Dabiri, "Performance enhancement of downstream vertical-axis wind turbines," *Journal of Renewable and Sustainable Energy*, vol. 8, p. 053306, 2016.
- [17] S. Le Fouest and K. Mulleners, "The dynamic stall dilemma for vertical-axis wind turbines," *Renewable Energy*, vol. 198, 08 2022.
- [18] M. Shiono, K. Suzuki, and S. Kiho, "An experimental study of the characteristics of a Darrieus turbine for tidal power generation," *Electrical Engineering in Japan*, vol. 132, no. 3, pp. 38–47, 8 2000.
- [19] P.-L. Delafin, T. Nishino, L. Wang, and A. Kolios, "Effect of the number of blades and solidity on the performance of a vertical axis wind turbine," *Journal of Physics: Conference Series*, vol. 753, p. 022033, 09 2016.
- [20] W. McCroskey, "The phenomenon of dynamic stall," NASA TM-81264, Tech. Rep., 1981.
- [21] A. Laneville and P. Vittecoq, "Dynamic stall: The case of the vertical axis wind turbine," *Journal of Solar Energy Engineering, Transactions of ASME*, vol. 108, pp. 140–145, May 1986.
- [22] L. Daróczy, G. Janiga, K. Petrasch, M. Webner, and D. Thévenin, "Comparative analysis of turbulence models for the aerodynamic simulation of H-Darrieus rotors," *Energy*, vol. 90, pp. 680–690, 2015.
- [23] T. Maître, E. Amet, and C. Pellone, "Modelling of the flow in a Darrieus water turbine: Wall grid refinement analysis and comparison with experiments," *Renewable Energy*, vol. 51, pp. 497–512, 2013.
- [24] L. Daróczy, G. Janiga, and D. Thévenin, "Computational fluid dynamics based shape optimization of airfoil geometry for an H-rotor using a genetic algorithm," *Engineering Optimization*, vol. 50, no. 9, pp. 1483–1499, 2018.
- [25] Y. Chen, L. Kuang, J. Su, D. Zhou, Y. Cao, H. Chen, Z. Han, Y. Zhao, and S. Fu, "Investigation of pitch angles on the aerodynamics of twin-vawt under staggered arrangement," *Ocean Engineering*, vol. 254, p. 111385, 2022.
- [26] K. Hansen, N. Rostamzadeh, R. Kelso, and B. Dally, "Evolution of the streamwise vortices generated between leading edge tubercles," *Journal of Fluid Mechanics*, vol. 788, p. 730–766, 2016.
- [27] R. Pérez-Torró and J. Kim, "A large-eddy simulation on a deep-stalled aerofoil with a wavy leading edge," *Journal of Fluid Mechanics*, vol. 813, p. 23–52, 2017.
- [28] M. K. Rathore, M. Agrawal, and P. Baredar, "Pitch control mechanism in various type of vertical axis wind turbines: A review," *Journal of Vibration Engineering & Technologies*, vol. 9, pp. 2133–2149, 2021.
- [29] L. Lazauskas and B. Kirke, "Modelling passive variable pitch cross flow hydrokinetic turbines to maximize performance and smooth operation," *Renewable Energy*, vol. 45, pp. 41–50, 2012.
- [30] S. Hoerner, S. Abbaszadeh, T. Maître, O. Cleynen, and D. Thévenin, "Characteristics of the fluid–structure interaction within Darrieus water turbines with highly flexible blades," *Journal of Fluids & Structures*, vol. 88C, pp. 13–30, 04 2019.
- [31] S. Hoerner, S. Abbaszadeh, O. Cleynen, C. Bonamy, T. Maître, and D. Thévenin, "Passive flow control mechanisms with bioinspired flexible blades in cross-flow tidal turbines," *Experiments in Fluids*, vol. 62, no. 104, pp. 1–14, 2021.
- [32] P.-O. Descoteaux and M. Olivier, "Performances of vertical-axis hydrokinetic turbines with chordwise-flexible blades," *Journal of Fluids and Structures*, vol. 102, p. 103235, 2021.
- [33] B. Strom, S. Brunton, and B. Polagye, "Intracycle angular velocity control of cross-flow turbines," *Nature Energy*, vol. 2, 2016.
- [34] B. Paillard, J. Astolfi, and F. Hauville, "URANSE simulation of an active variable-pitch cross-flow darrieus tidal turbine: Sinusoidal pitch function investigation," *International Journal of Marine Energy*, vol. 11, pp. 9–26, sep 2015.
- [35] P.-L. Delafin, F. Deniset, J. A. Astolfi, and F. Hauville, "Performance improvement of a darrieus tidal turbine with active variable pitch," *Energies*, vol. 14, no. 3, p. 667, jan 2021.
- [36] S. Abbaszadeh, S. Hoerner, T. Maître, and R. Leidhold, "Experimental investigation of an optimised pitch control for a vertical-axis turbine," *IET Renewable Power Generation*, vol. 13, pp. 3106–3112(6), 2019.
- [37] T. Bennecke, K. Ruiz-Hussmann, P. Joedecke, C.-T. Weber, P.-L. Delafin, C. Bonamy, and S. Hoerner, "A weak coupled model for the fluid-structure interactions on cross-flow tidal turbine model," in *The 8th European Congress of Computational Methods in Applied Sciences and Engineering ECCOMAS Congress 2022, Oslo, Norway*, 2022.
- [38] T. Bennecke, S. Abbaszadeh, K. Ruiz-Hussmann, P. Joedecke, P.-L. Delafin, C.-T. Weber, and S. Hoerner, "A methodology to capture the single blade loads on a cross-flow tidal turbine flume model," in *Proceedings of the 15th European Wave and Tidal Energy Conference, 3–7 September 2023, Bilbao*, 2023.
- [39] P.-L. Delafin, S. Guillou, J. Sommeria, and T. Maitre, "Mesh sensitivity of vertical axis turbine wakes for farm simulations," in *24th Congrès Français de Mécanique*, 2019.
- [40] S. Hoerner, C. Bonamy, O. Cleynen, T. Maître, and D. Thévenin, "Darrieus vertical-axis water turbines: deformation and force measurements on bioinspired highly flexible blade profiles," *Experiments in Fluids*, vol. 61, no. 141, 2020.
- [41] Z. Zhao, S. Hoerner, and R. Leidhold, "Intracycle active blade pitch control for cross-flow tidal turbines using embedded electric drive systems," in *Proceedings of the 15th European Wave and Tidal Energy Conference, 3–7 September 2023, Bilbao*, 2023.

- [42] —, “Design and analysis of a blade-embedded limited-angle torque motor for vertical-axis water turbines,” in *11th International Conference on Power Electronics, Machines and Drives*, 2022.
- [43] L. Daróczy, G. Janiga, and D. Thévenin, “Systematic analysis of the heat exchanger arrangement problem using multi-objective genetic optimization,” *Energy*, vol. 65, pp. 364–373, 2014.
- [44] E. Kerikous and D. Thévenin, “Optimal shape of thick blades for a hydraulic Savonius turbine,” *Renewable Energy*, vol. 134, pp. 629 – 638, 2019.
- [45] T. Parikh, M. Mansour, and D. Thévenin, “Maximizing the performance of pump inducers using cfd-based multi-objective optimization,” *Structural and Multidisciplinary Optimization*, vol. 65, 2022.
- [46] K. Ruiz-Husmann, P.-L. Delafin, C. Bonamy, Y. Delannoy, D. Thévenin, and S. Hoerner, “Blade shape optimisation of a vertical axis tidal turbine under constraints,” in *Proc. Conference on Modelling Fluid Flow (CMFF’22) in Budapest, Hungary*, 2022, pp. 420–426.
- [47] —, “Objective functions for the blade shape optimization of a cross-flow tidal turbine under constraints,” in *Proceedings of the 15th European Wave and Tidal Energy Conference, 3–7 September 2023, Bilbao*, 2023.
- [48] O. Cleynen, S. Engel, S. Hoerner, and D. Thévenin, “Optimal design for the free-stream water wheel: A two-dimensional study,” *Energy*, vol. 214, p. 118880, 2021.
- [49] F. Guillaume, M. Sacher, F. Hauville, J.-A. Astolfi, and G. Germain, “Multi-objective optimization of cycloidal blade-controlled propeller: an experimental approach,” *preprint*, 04 2023. [Online]. Available: https://www.researchgate.net/publication/369795243_Multi-objective_optimization_of_cycloidal_blade-controlled_propeller_an_experimental_approach
- [50] K. Deb, A. Pratap, S. Agarwal, and T. Meyarivan, “A fast and elitist multiobjective genetic algorithm: NSGA-II,” *IEEE Transactions on Evolutionary Computation*, vol. 6, no. 2, pp. 182–197, 2002.